Experimental investigation of laser cladding of H13 hot work steel by Stellite 6 powder

MEHDI SAFARI*,[1], MAHMOUD MORADI[2], JALAL JOUDAKI[1], AMIR MOHAMMAD BABAEI[1]

[1] Department of Mechanical Engineering, Arak University of Technology, Arak 38181-46763, Iran
[2]School of Mechanical, Aerospace and Automotive Engineering, Faculty of Engineering, Environment and Computing, Coventry University, Gulson Road, Coventry CV1 2JH, United Kingdom
e-mail: m.safari@arakut.ac.ir

Abstract. Cladding of metals can enhance the wear behavior of metals. Many dies work at elevated temperature such as hot forging dies and hot extrusion dies needs resistance to wear at higher temperatures. In this article, the cladding of H13 hot work steel (DIN 1.2324) will be investigated by laser cladding. The Stellite 6 powders coat the steel surface by using a continuous fiber laser. Two important objects in cladding are the effect of laser process parameters on the quality of the cladding layer and the lateral overlapping percent in adjacent passes. The laser power, scanning speed, and powder feed rate are the process variables in the study. The results show that the laser power is the most influencing parameter and by increasing laser power and decreasing the scanning speed, the hardness and penetration depth of cladded powder in the substrate will be increased. The dilution factor increases by increasing the laser power and reducing scanning speed at a moderate powder feed rate. The microstructure observation shows that strong metallurgical bonding between the clad and substrate and good mixing of powder in substrate metal can be obtained by proper setting of process parameters. The micro-hardness of the cladded specimen increased 300 HV (164 % increase compared to the substrate material. Best results were obtained at 10 % overlapping between adjacent irradiation passes.

Keywords. Laser Cladding; Stellite 6; H13 tool steel; Clad Geometry; Dilution.

1. Introduction

Surface treatment is important in manufacturing. Desired properties such as resistance to wear can enhance the duration life of fabricated parts. Laser cladding is a new and advanced surface treatment method that was recently used for enhancing fatigue life and wear resistance. The metallic powder melts by irradiated heat of the laser beam and produces a uniform cladding on the surface [[1]]. Different metallic powders can be deposited on the base metal. The thickness of the cladded layer is about 0.5 to 2 mm with a narrow width of

* For correspondence

about 0.4 mm. The conventional substrate materials are steel, cast iron, titanium alloys, aluminum alloys, magnesium alloys, and copper alloys. The laser cladding process can create a strong coating with a low dilution factor, good metallurgical bonding between the cladded layer and substrate, less distortion, narrow heat-affected zone, high cooling rate, and solidification.

Several pieces of research have been conducted to investigate different aspects of laser cladding. Naghiyan Fesharaki *et al* [[2]] compared the microstructure of laser-cladded and TIG (Tungsten Inert Gas) cladded specimens by Inconel 625 powder. The results show that dendritic growth of gains underneath the cladding surface. Moradi and Arabi *et al* [[3]] investigated the surface hardening of AISI 410 steel by a laser beam using the response surface methodology. The results show that the hardness and penetration depth of the cladded specimen increased by increasing the laser power and decreasing the scanning speed. Bhatnagar *et al* [[4]] studied the laser cladding of AISI 304 stainless steel by Inconel 625 powder. The Inconel 625 powder was placed and covered the surface of the substrate before starting the laser irradiation. A lumped parametric analytical model has been developed for the prediction of the molten pool temperature, clad geometry, and dilution. Energy transfer and loss mechanisms are two main important phenomena in the model. Wu *et al* [[5]] studied the effect of process parameters of laser cladding using the response surface methodology. The substrate was 42CrMo steel and the powder was Ni60A-25% tungsten carbide (WC) powder. A significant increase in the micro-hardness was observed due to the formation of the martensite phase within the cladded surface. Liu *et al* [[6]] studied the effect of Ti content on the wear resistance of cladded austenite stainless steel by the laser beam. The cladding powder was FeCoNiCrMnTi. Experimental results show that the Ti element combined with high purity N2 shielding gas and produces TiN particles in situ. The TiN particle improved the wear resistance of the coating by about 1.9 times.

Yang *et al* [[7]] investigated the cladding of 45# steel substrate by FeCrMoMn coatings. The laser cladding has been carried out at the scanning speed of 0.4 m/min, 40 m/min, and 70 m/min, respectively. The results show that laser cladding at higher speeds decreases grain size, heat-affected zone, and dilution due to solute trapping of the coat. Metallurgical bonding is created between the substrate and the coat. Considerable improvement in the hardness and electrochemical corrosion resistance was observed. Lizzul *et al* [[8]] studied the laser cladding of C45 steel substrates were laser cladded with multiple layers of AISI H13 tool steel. The effect of main process parameters (powder granulometry, scanning speed, laser power, and the number of deposited layers) were investigated to achieve a dense and

homogeneous cladding layer with high hardness. The results showed that, for the first time, a robust correlation exists between the number of layers and the cladding characteristics. Increasing the number of cladded layers improves the machinability of cladded substrate.

Cheng *et al* [[9]] studied the underwater laser cladding of aluminum alloy. The results show that the height of the cladding zone and the cladding angle increased, but the width of the cladding zone and the depth of the melting zone decreased. Much smaller columnar dendrites and equiaxial dendrites were observed in the water environment. Intermetallic compounds (Al0.5Fe3Si0.5) formed in both underwater and in-air cladding zone but the formation of intermetallic compounds was reduced in the water environment. The water environment increases magnesium content and helps the refinement of microstructure.

Karmakar *et al* [[10]] compared the high-temperature abrasive wear behavior of H13 steel surfaces modified by laser remelting and cladding with Stellite 6 and Stellite 6 + 30 wt% WC. The results show that laser remelting can prepare higher hardness than laser cladding of Stellite 6 powders but the Stellite 6/WC composite clad layer had considerably higher hardness than the Stellite 6 cladded powder. Also, a relatively less volumetric loss was observed for the cladded Stellite 6/WC layer in abrasive wear. Karmakar *et al* [[11]] studied the bond strength of laser cladded Stellite 21 layers deposited on AISI H13 tool steel. The results show that parallel scanning paths can generate higher bonding between the cladded layer and the substrate and increasing the energy leads to higher bond strength because of a more uniform overlapped clad interface. Lu *et al* [[12]] studied repairing the damaged components of H13 tool steel by the Ni25 laser cladding and consequent laser shock peening. The results showed that after the laser shock peening process, columnar dendrites on the surface transformed into refined equiaxed dendrites and compressive residual stresses induced on the surface of the specimen. In addition, the friction coefficient and wear rate of Ni25 coating were decreased significantly.

Telasang *et al* [[13]] examined the laser cladding of AISI H13 tool steel powder on AISI H13 tool steel components using a 6kW diode laser. The maximum increase in hardness was 650VHN (about a 45% increase). Laser reheating (tempering) of the cladded layer with a 1000W laser power showed a more refined microstructure with maximum hardness up to 680–700VHN. Several studies have been done on laser cladding of H13 steel. Hao *et al* [[14]] investigated the laser cladding of Inconel 625 on the H13 mold steel. Lei *et al* [[15]] used NiCrBSi+Ni/MoS2 powders for laser cladding of H13. Xue *et al* [[16]] cladded H13 steel with Ni25/Fe104 composite powder. Kattire *et al* [[17]] used CPM 9V steel powder for repairing the damaged H13 tool steel die surfaces.

The above articles show the significance of laser cladding of H13 tool steel. The H13 tool steel is usually used for the fabrication of dies at elevated temperatures. Despite the interest and application of H13 tool steel at elevated temperatures, limited research was published on the properties of laser-cladded H13 tool steel. A literature survey demonstrates that laser cladding can be used in industries to enhance the life of dies in manufacturing. Forging dies, hot extrusion dies and other forming processes at elevated temperatures can be good examples of laser cladding of H13 hot work steel. The authors had preceding experiments on the cladding of Stellite 6 powder on H13 tool steel. The cladding was done by other manufacturing processes but the authors believe that the concentrated energy emitted by the laser beam can enhance the surface integrity of cladded specimens more effectually. In this study, the laser cladding of H13 tool steel by Stellite 6 powder will be investigated experimentally. The main novelty of the current work is using Stellite 6 powder as a commercially and widely used coating for cladding of H13 tool steel to create a suitable cladding. The effect of process parameters (laser power, scanning speed, and powder feed rate) on the quality of cladding will be investigated. Cladded layer height, width, and dilution factor will be measured and the best condition for lateral overlapped cladding will be obtained.

2. Experimental procedure

2.1. Experimental setup

Figure 1 shows a schematic illustration of the laser cladding process. The powder feeds through a nozzle on the surface of the base material and melts by the laser-irradiated beam. The substrate was prepared from H13 hot work steel (also known as DIN 1.2334, SKD61, X40CrMoV5-1 in other standards) which is used widely for the fabrication of hot forge and hot extrusion dies. The chemical composition of H13 tool steel and Stellite 6 powder was reported in table 1 (measured by quantometer machine). The H13 tool steel contains Cr, Mo, V, and Si elements that increase the resistance to wear, resistance to thermal shock, and the ability to maintain mechanical properties at high temperatures. It is used widely in die fabrication. The cladding layer is Stellite 6 powder which is a Cobalt base alloy. Cladding by Stellite 6 is usually carried out when high strength, high corrosion resistance, and high resistance to wear are needed [[18]]. The cladded surface by Stellite 6 needs low lubrication in metal-to-metal contact and consequently low friction coefficient. The used powder

contains spherical dots with 10-40 µm diameter and is suitable for cladding of surfaces. Figure 2 shows the scanning electron microscopic (SEM) image of the used powder.

Table 1. Chemical composition of the Stellite 6 powder and H13 tool steel.

Element	Co	Cr	W	Ni	Fe	Mn	C	Si	V	Mo
Powder (wt. %)	Bal.	31	4.6	2.0	1.01	1.22	1.2	1.02	-	0.55
H13 tool steel (wt. %)	-	5.16	-	0.35	Bal.	0.38	0.39	1.03	0.95	1.38

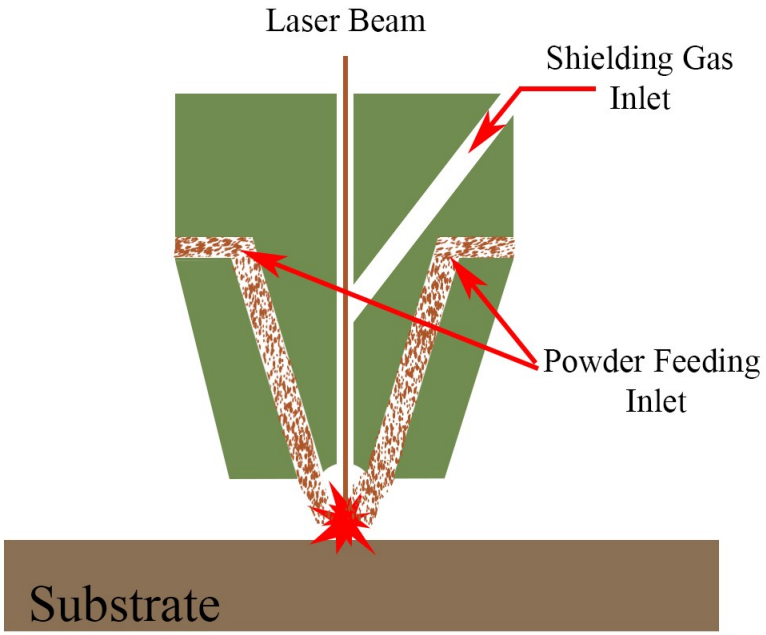

Figure 1. Schematic illustration of laser cladding of the Stellite 6 powder.

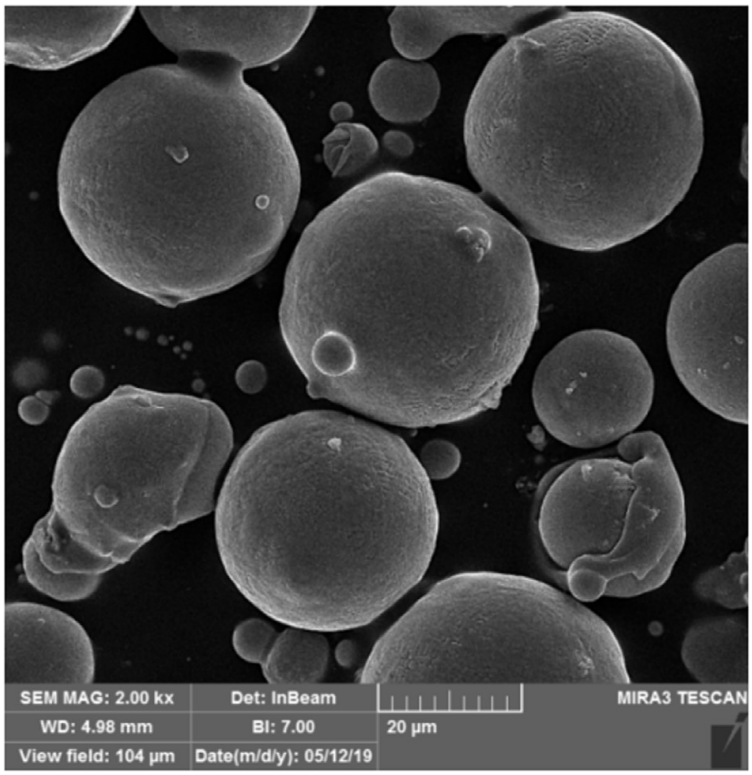

Figure 2. SEM image of Stellite 6 powder used for laser cladding [[19]].

The laser cladding was implemented by a 1 kW continuous fiber. The focal length of the laser was 4 mm and Argon gas was used as shielding gas. The shielding gas is blown coaxially with the laser beam. A specific nozzle has been designed and fabricated to deliver the Stellite 6 powder to the beam irradiation point. This nozzle has four grooves to guide the powder properly. A subsidiary groove for shielding gas is also located in this nozzle which can be seen in Figure 1.

2.2. Experimental tests

Rectangular plates from H13 hot work steel prepared by saw cutting (50×20×8 mm dimensions). The surface of the prepared plate was polished, degreased, and washed with acetone. The plate was fixed in a specified position by a fixture and after tuning the laser machine, the laser cladding of the plate started. The laser source is perpendicular to the top surface. The experimental test will study the effect of process parameters on the geometrical dimension of the cladded layer and also the percent of side overlapping to fabricate a proper surface cladding. Table 2 shows the implemented experiments obtained by Taguchi's design of experiments method. In this article, four different powder feed rates including 21, 24, 27, and 30 g/min will be studied.

Table 2. Designed experiments for laser cladding of H13 tool steel.

Sample ID	Laser Power (W)	Scanning Speed (mm/min)	Powder Feed Rate (g/min)
A1	250	150	24
A2	250	150	30
A3	250	300	24
A4	250	300	30
A5	250	150	27
A6	300	150	30
A7	300	150	24
A8	300	150	27
A9	300	250	27
A10	250	300	27
A11	300	150	21
A12	350	250	27
A13	350	150	27
A14	350	150	24

The shielding gas flow, focal plane position (FPP), and flow of powder-carrying gas keep constant during the experiments. Their value is 3 lit/min, 4 mm, and 1.5 lit/min respectively. A straight line was cladded on the top surface of the plate and the plate was left for 120 seconds for cooling before starting the next pass of irradiation. The next line will be cladded with new configurations. Figure 3 shows the macro image of the cross-section of cladded specimens. The height and width of the deposited layer and penetration depth were measured in an optical microscope using ImageJ software [[20]]. Some cracks and porosities have been observed in the cladded specimens which relate to high-temperature gradient variation in laser cladding. The cladded specimens were cut at a 15 mm distance from the start point of cladding by an electro-discharge machining (EDM) machine. The specimens were mounted and polished with sandpaper. The prepared samples were used for metallography observation and surface hardness measurement. A micro-hardness testing machine was used, and the Vickers hardness was measured by applying 100 g force and holding time 10s. The hardness was measured in polished cross-section (from cladded layer to substrate) underneath the surface. In addition, for measuring the hardness profile along with the thickness, hardness tests have been carried out by applying 10 g force.

The specimen was etched chemically by Nital and Glycirage etchant to observe the microstructure of cladded specimens. Figure 4 shows a schematic view of the cladded surface. The width of the deposited layer (W), the height of the deposited layer (h), and the penetration depth in the substrate (d) will be measured in cladded specimens. The dilution is an important parameter in determining the quality of the cladded surface [[1]]. The dilution

factor is defined as the amount of intermixing of the cladded layer and the substrate material. The dilution affects the mechanical behavior of the sample. The dilution factor (D) according to the shown parameters in Figure 4 is defined as equation (1).

$$D = \frac{d}{d+h} \times 100 \tag{1}$$

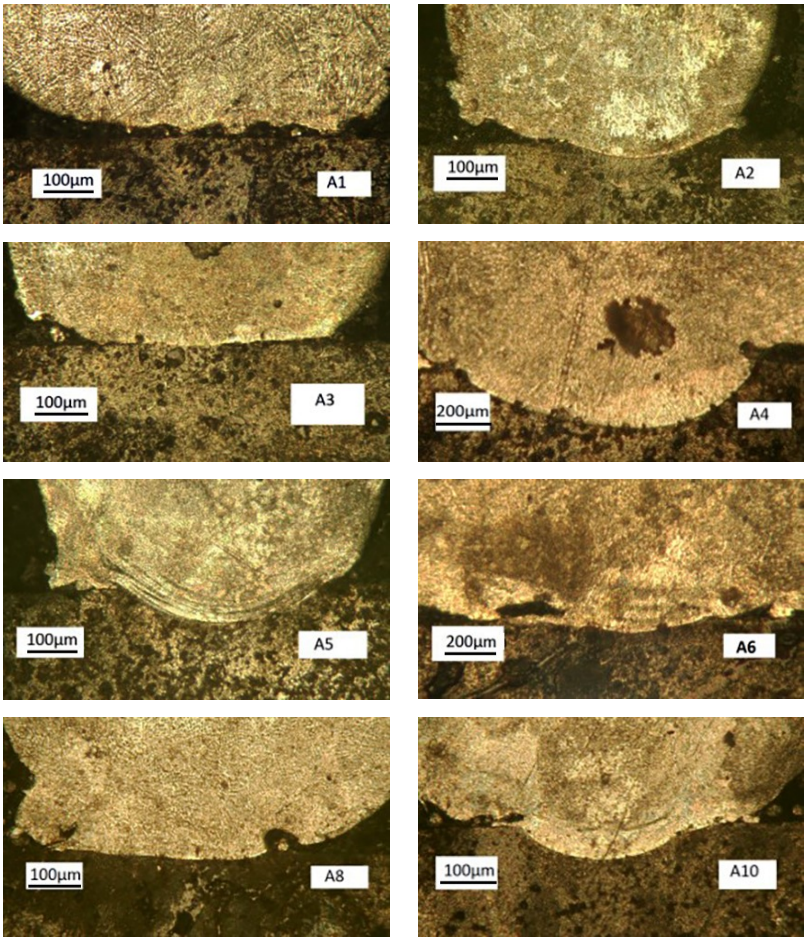

Figure 3. Cross-section of some cladded specimens.

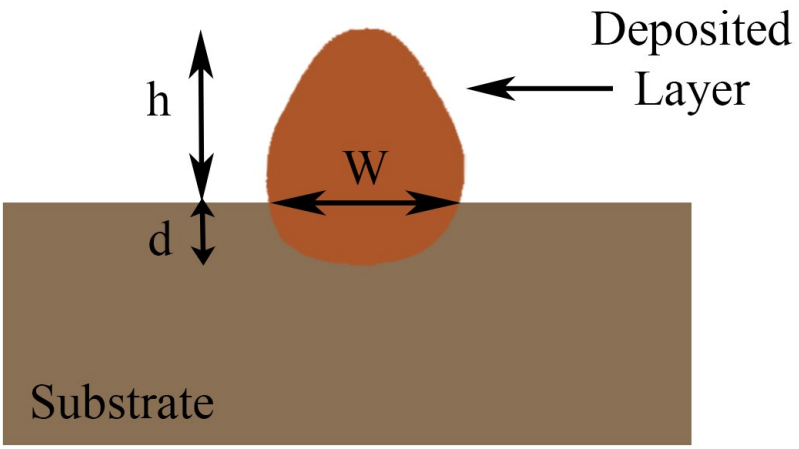

Figure 4. Schematic view of cladded specimen.

3. Results and discussion

3.1. Dilution of the cladded layer

Figure 5 shows the variation of dilution factor according to laser cladding process parameters (laser power, scanning speed, and powder feed rate). The results show that the dilution factor increases by increasing the laser power. The absorbed energy by the powder and workpiece increases by increasing the laser power and consequently, the penetration depth of cladded powder increases, and a higher dilution factor will be obtained for laser cladding.

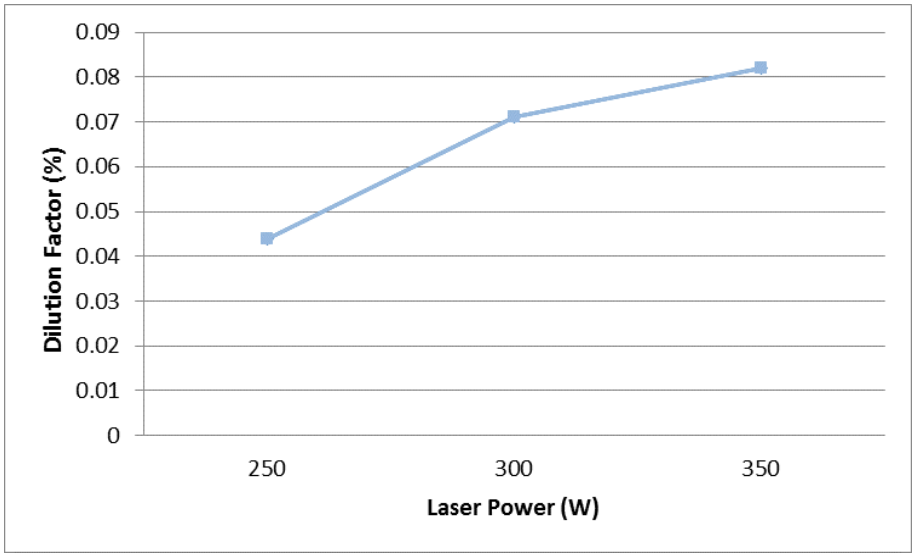

(a)

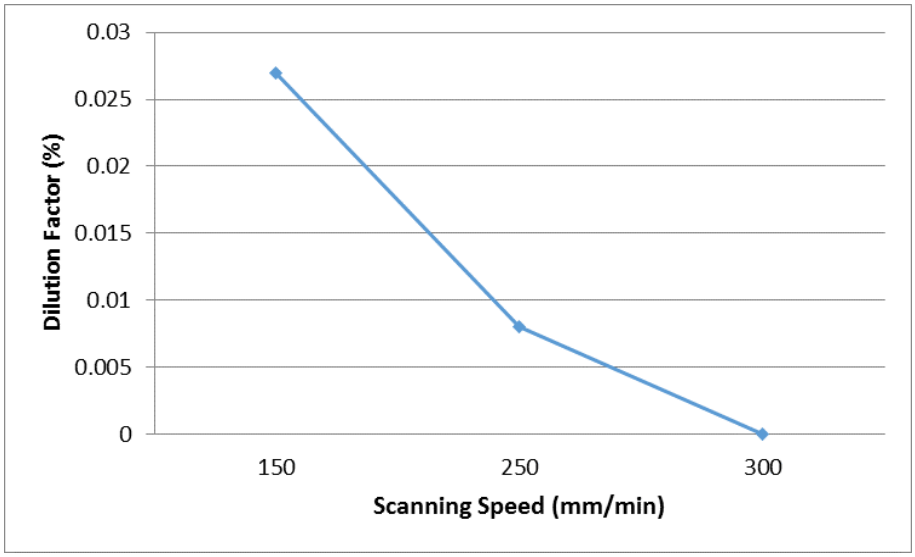

(b)

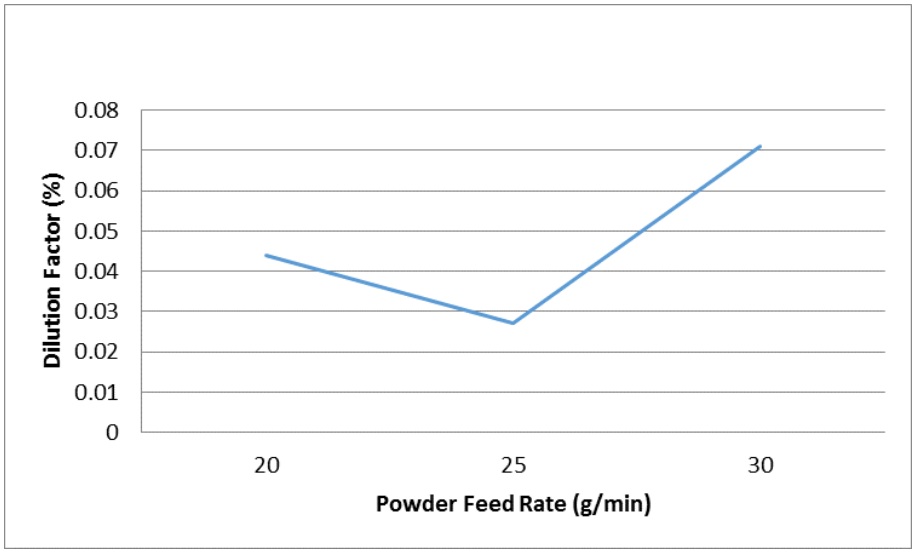

(c)

Figure 5. Variation of dilution factor by (a) laser power, (b) scanning speed, (c) powder feed rate.

As can be seen in Figure 5(b), the dilution factor decreases by increasing the scanning speed of the laser. By increasing scanning speed, the absorbed energy decreases and generated heat per unit length decreases which leads to a low dilution factor. Increasing scanning speed to 300 mm/min decreases the dilution factor to zero value and means no intermixing between the powder and substrate. So, practically, the cladding layer separates from the substrate very easily and bad cladding happens. Figure 5(c) shows that increasing powder feed rate firstly

leads to decreasing dilution factor then it increases due to entering more powder in melting zone and intermixing of powder and substrate increases.

3.2. Geometry of the cladded layer

Figure 6 shows the effect of laser power on the geometry of the cladded layer. The powder feed rate and scanning speed were constant during the investigation (27 g/min and 150 mm/min respectively). The results show that by increasing the laser power, more powder will melt, and the width and height of the cladded layer will increase firstly and then decrease.

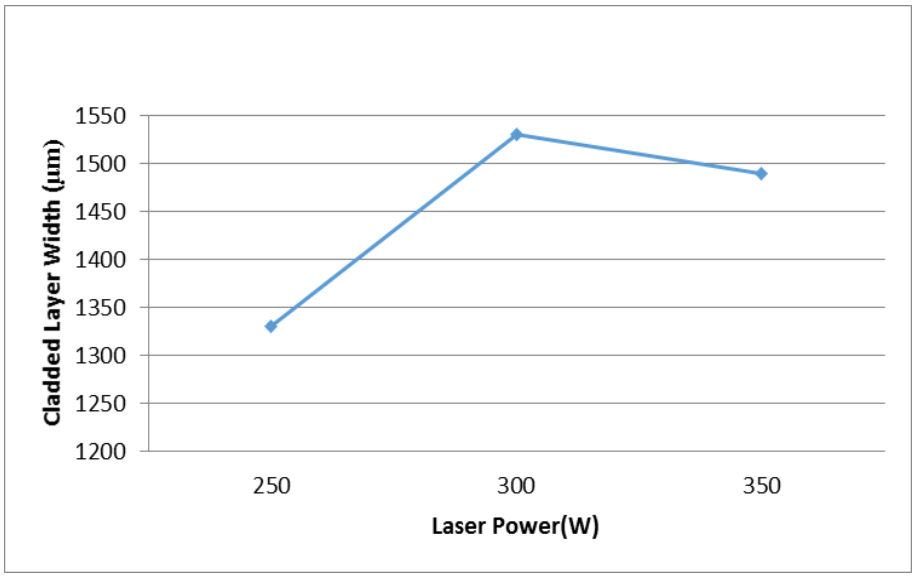

(a)

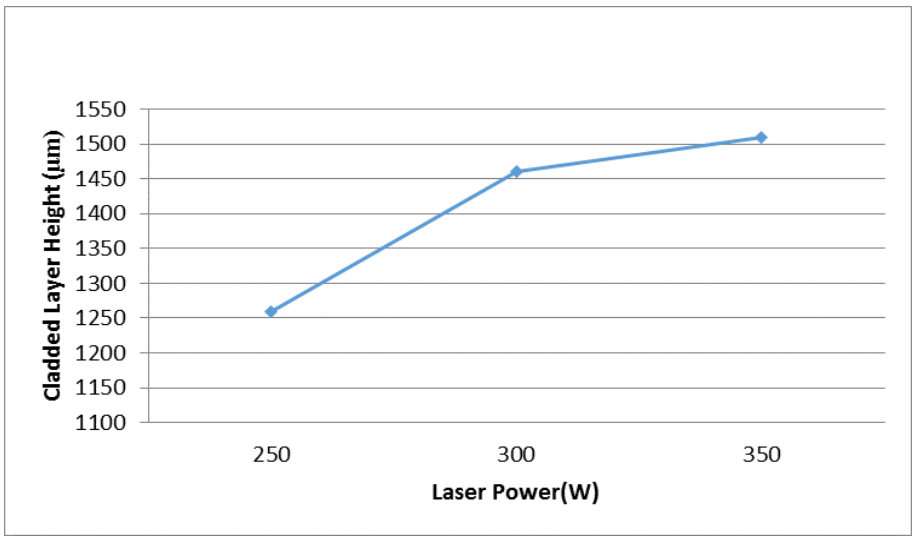

(b)

Figure 6. Effect of laser power on a) cladded layer width b) cladded layer height.

Increasing dilution at higher laser power leads to a higher penetration depth in the substrate and the width of the cladded layer decreases a little. Figure 7 shows the effect of scanning speed on the geometry of the cladded layer. The laser power and powder feed rate were 300 W and 24 g/min respectively. By increasing the scanning speed, the absorbed energy per unit of length decreases, So, the width of the cladded layer will decrease. Also, the penetration depth decreases which shows lower melting of power during the process. The height of the cladded layer decreases by increasing scanning speed. So, the width and height of the cladded layer will decrease, and a thinner and weaker cladded layer will be obtained.

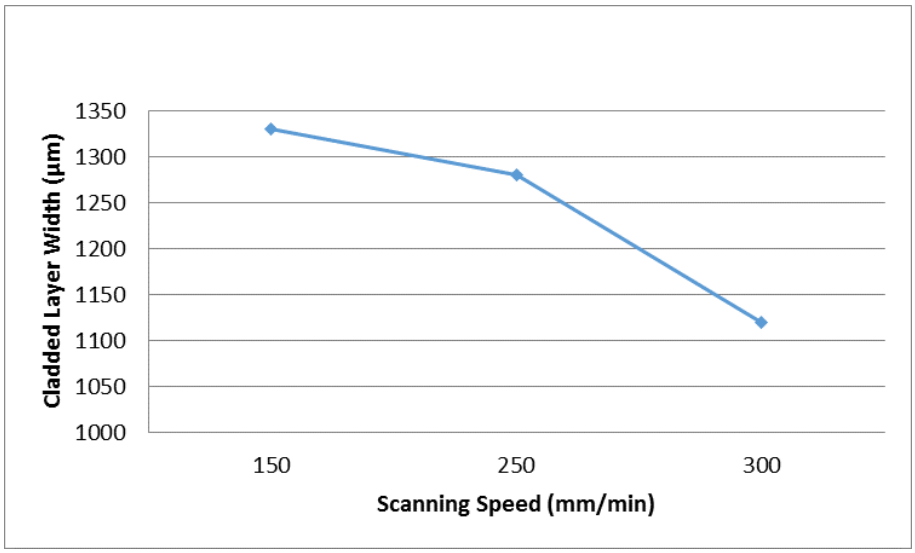

(a)

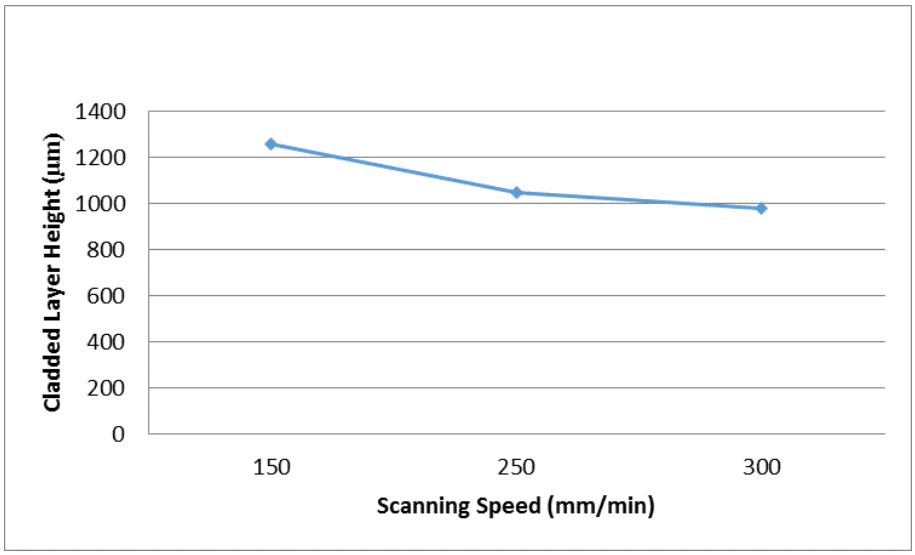

(b)

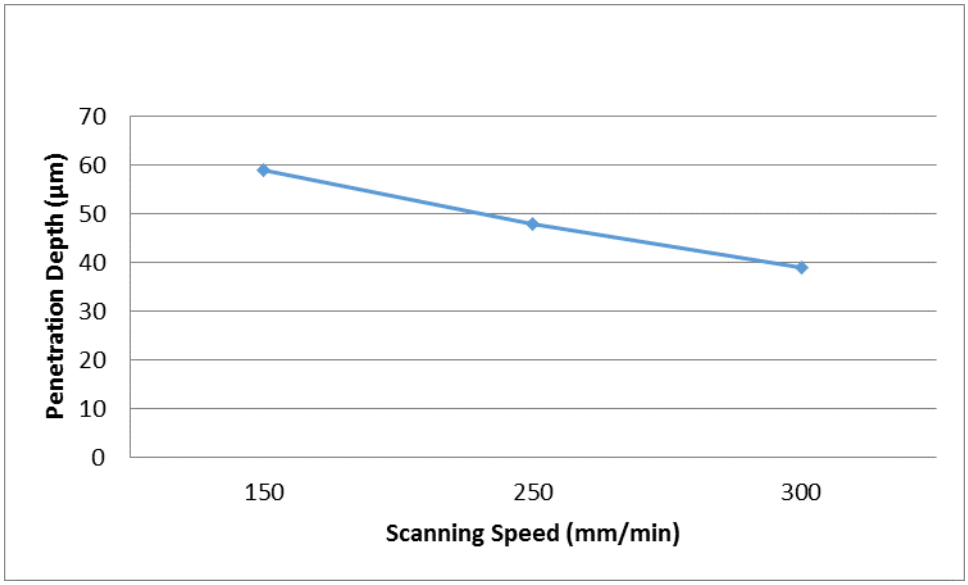

(c)

Figure 7. Effect of scanning speed on (a) layer width, (b) layer height, (c) penetration depth.

Similar results had been observed in the powder feed rate. Figure 8 shows the effect of powder feed rate variation in laser cladding. The results show that by increasing the power feed rate, the width and height of the cladded layer decrease. The penetration depth in the substrate decreases which means lower dilution of the cladded layer. A higher powder feed rate needs a higher value of laser power to melt the powder and substrate.

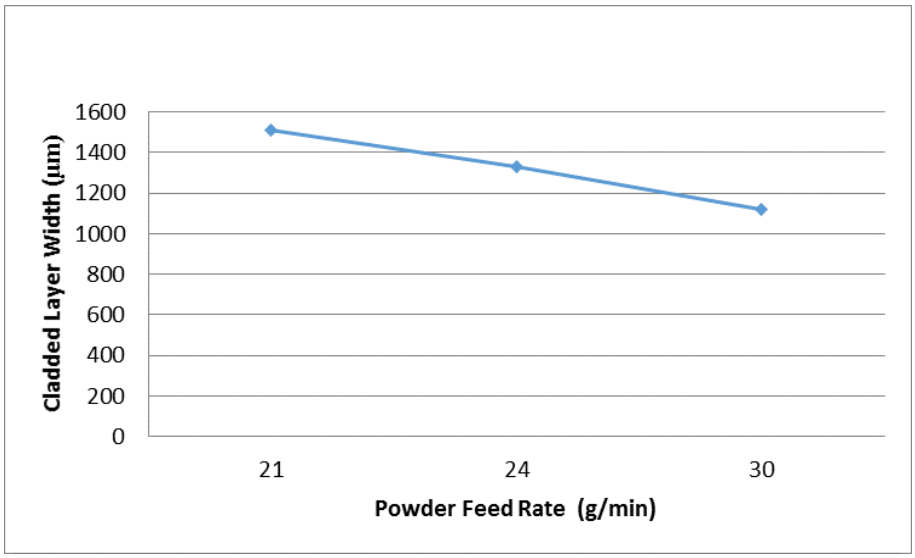

(a)

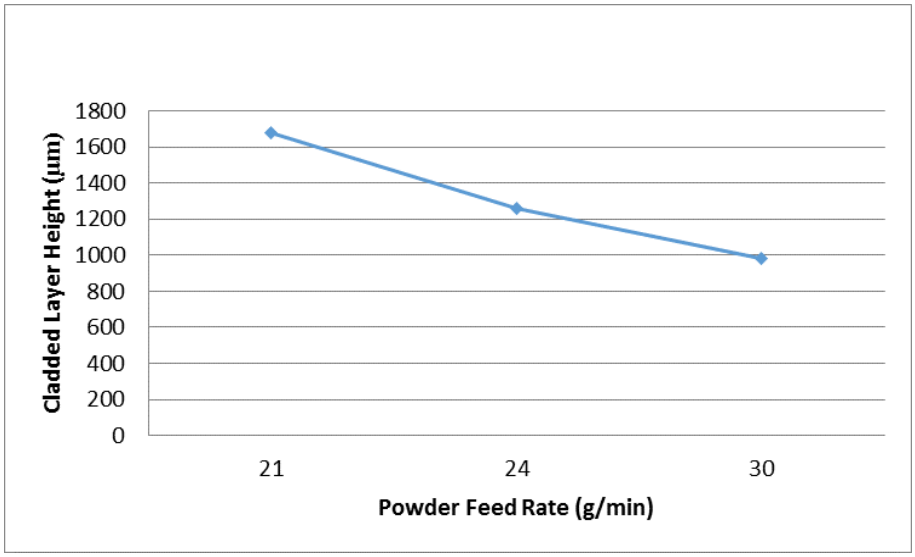

(b)

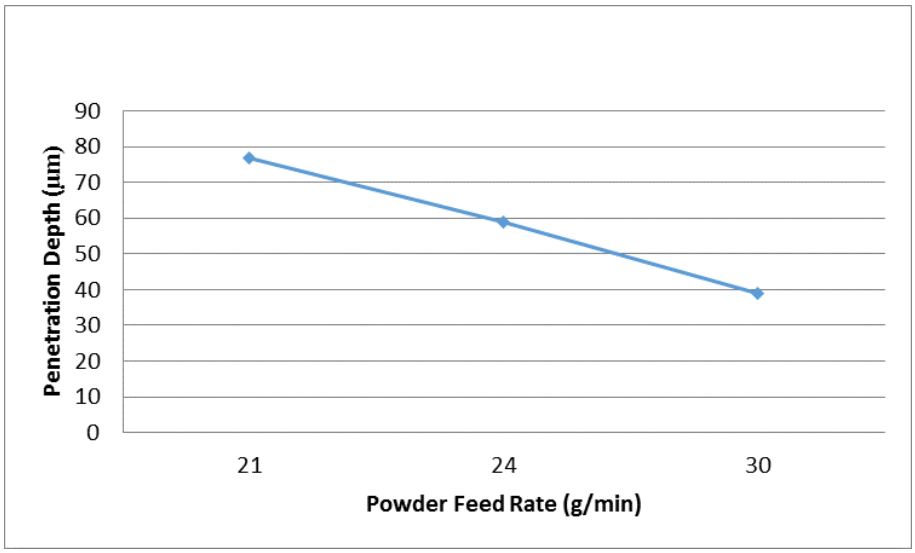

(c)

Figure 8. Effect of powder feed rate on (a) layer width, (b) layer height, (c) penetration depth.

At last, it can be concluded that a strong, high diluted, and thicker cladding layer can be obtained by increased laser power and lower scanning speed and powder feed rate. The penetration depth of the cladded layer is important and higher penetration depth leads to higher dilution and a more desired cladding layer.

3.3. Lateral overlapping

The overlapping of cladding passes is important in laser cladding. The process parameters were tuned as 300 W laser power, 150 mm/min scanning speed, and 30 g/min powder feed rate. Figure 9 shows the cross-section of overlapped layers. The laser beam diameter was 0.5 mm and 40%, 30%, 10%, and 0% overlapping were examined. The distance between the parallel irradiating paths sets by $(100 - \text{overlapping percentage}) \times \text{beam diameter}$. The microscopic results show that no lateral overlapping happens in 0% overlapping and mixing of the melted layers happens and some porosities were observed in 30% and 40% overlapping. The best results were observed in 10% lateral overlapping.

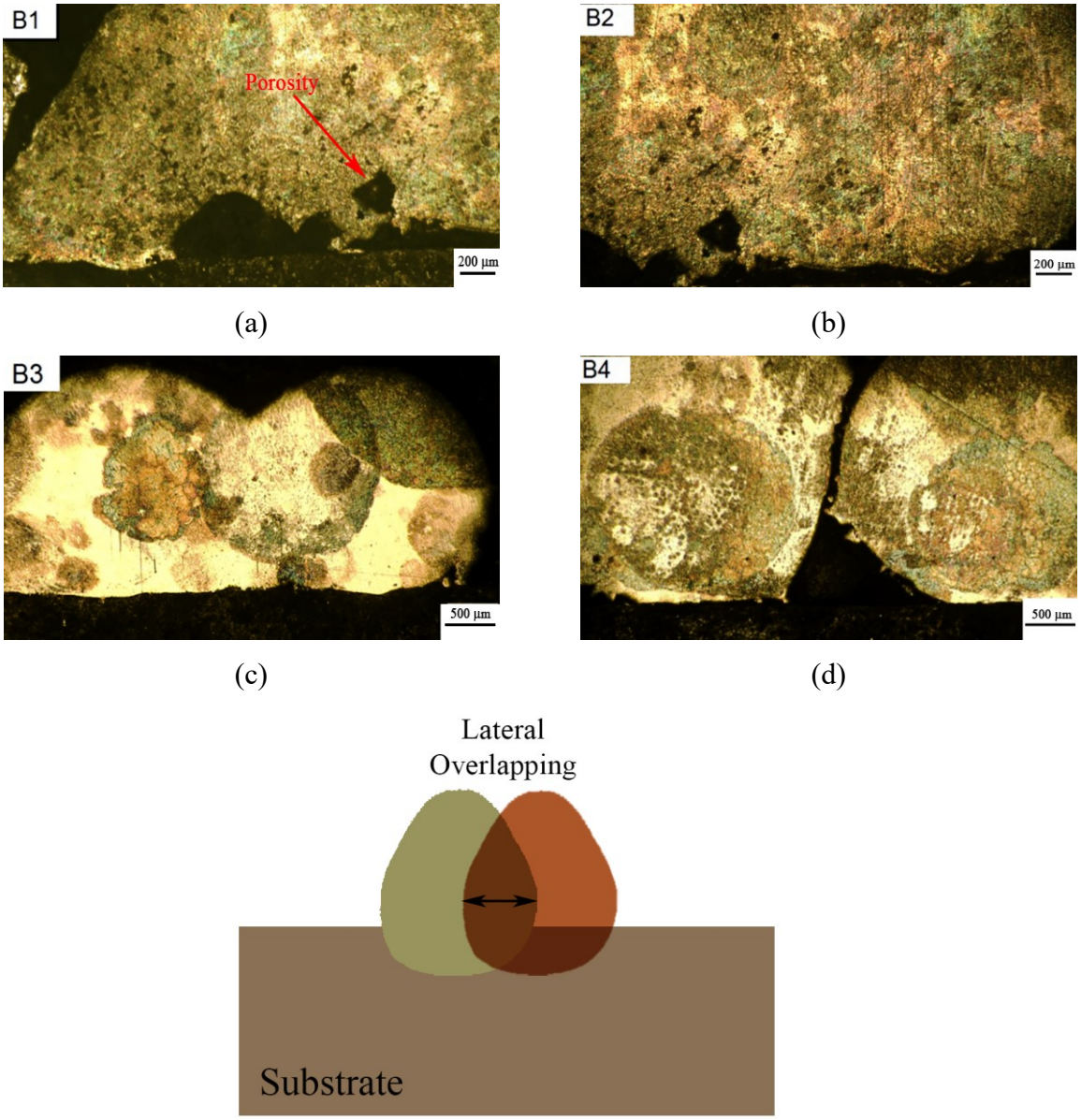

Figure 9. Cross-section of cladded passes with (a) 40%, (b) 30%, (c)10%, (d) 0% overlapping (no overlapping), (e) schematic illustration of lateral overlapping.

3.4. Microstructure observation and micro-hardness result

Figure 10(a) shows the microstructure of Stellite 6 cladded layer (front view) observed in an optical emission microscope (OEM). Two different phases have been observed, Cobalt dendritic grains (white zones) and Carbide precipitates zones (black zones). Figure 10(b) shows the side view of the cladded specimen. The microstructure changes from columnar to cell, then dendritic, and at last equiaxed grains. The cooling speed in the molten pool is high and coarse columnar crystals form along the normal direction of grains. By decreasing the solidification speed, dendritic grains grow. Part of the substrate melts and equiaxed grains can be observed. Figure 11 shows the overall view of the cladded layer and the substrate. Epitaxial growth of grains underneath the cladded layer can be observed obviously.

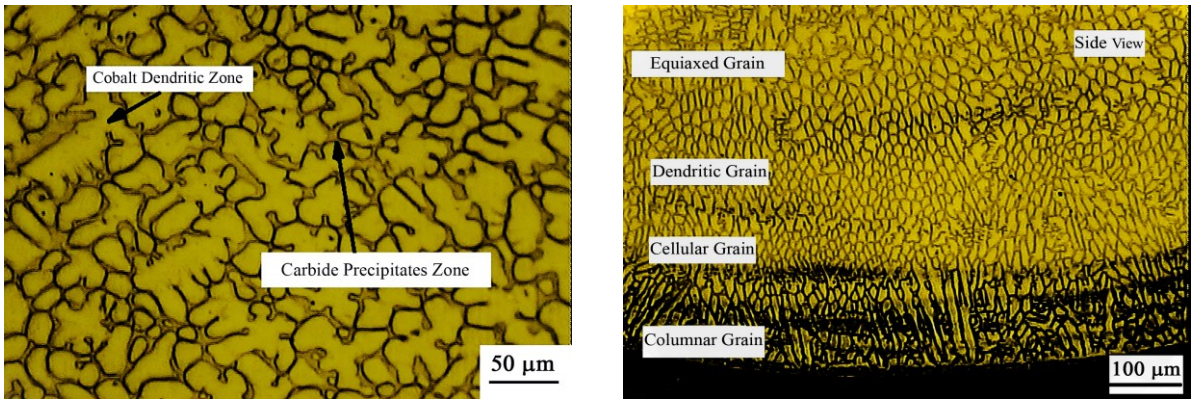

(a) (b)

Figure 10. Microstructure of cladded specimen (a) front view, (b) side view.

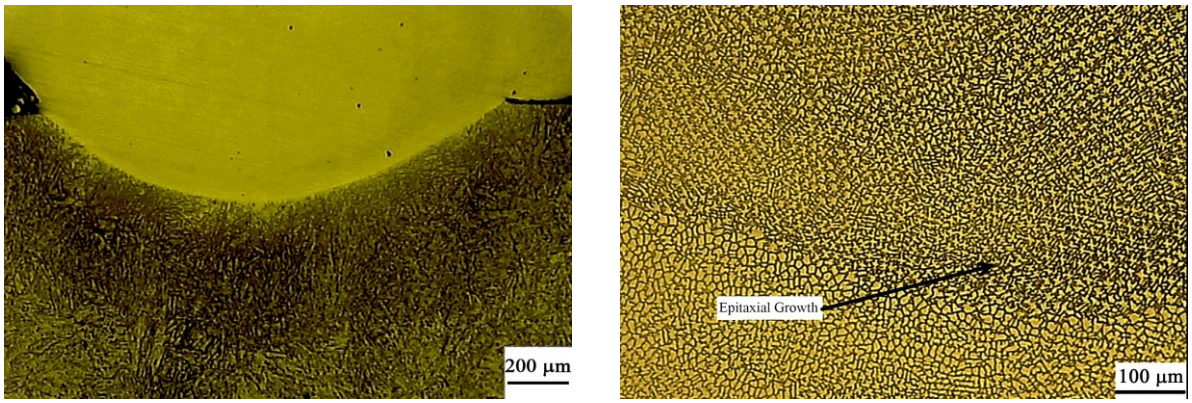

(a) (b)

Figure 11. (a) The grain growth at the boundary of the cladded layer and substrate, (b) The epitaxial growth at the boundary of the cladded layer and the substrate.

The epitaxial growth of dendritic grains causes a more strengthened joint between the cladded layer and the substrate. The substrate material is hot work steel and its crystal structure is BCC and the Stellite 6 has also a similar structure at below melting temperature. So, during the cooling of the molten pool, a good joining of structures will be obtained. The high cooling rate of the molten pool prevents the formation of nucleation of new grains and dendritic growth of grains will be observed in the cladded layer. Similar to the welding process, melting of the surface will lead to changes in the residual stress distribution. The graphs of penetration depth show that the thickness of penetration depth in all cladding samples is between 40-70 μm. Also, the micrograph of the boundary of the cladded layer and substrate shows that the thickness of heat affected zone is about 600 μm. The laser cladding will lead to tensile residual stresses on the surface of the cladded sample and the proper method for measuring the residual stress is the X-Ray diffraction method.

Figure 12(a) shows the measured micro-hardness results along the cross-section of the cladded sample. The substrate metal has 198 HV hardness and the hardness increases to 524 HV in the Stellite 6 cladded layer (164% increase in hardness). The hardness variation in the cladded layer is negligible (±15 HV). The hardness in the heat-affected zone (HAZ) increased compared to the substrate because of recrystallization and the formation of refined grains. Figure 12(b) shows the profile of micro-hardness along with the depth at the cross-section of the cladded sample. As can be seen, the hardness decreases from about 550 HV at Stellite 6 powder to about 300 HV in the mixture zone of Stellite 6 and H13 tool steel, and then it decreases to about 200 HV which is the hardness of the substrate (base) metal. Little changes were observed between Figure 12(a) and Figure 12(b) due to different applied loads in the micro-hardness measurement test.

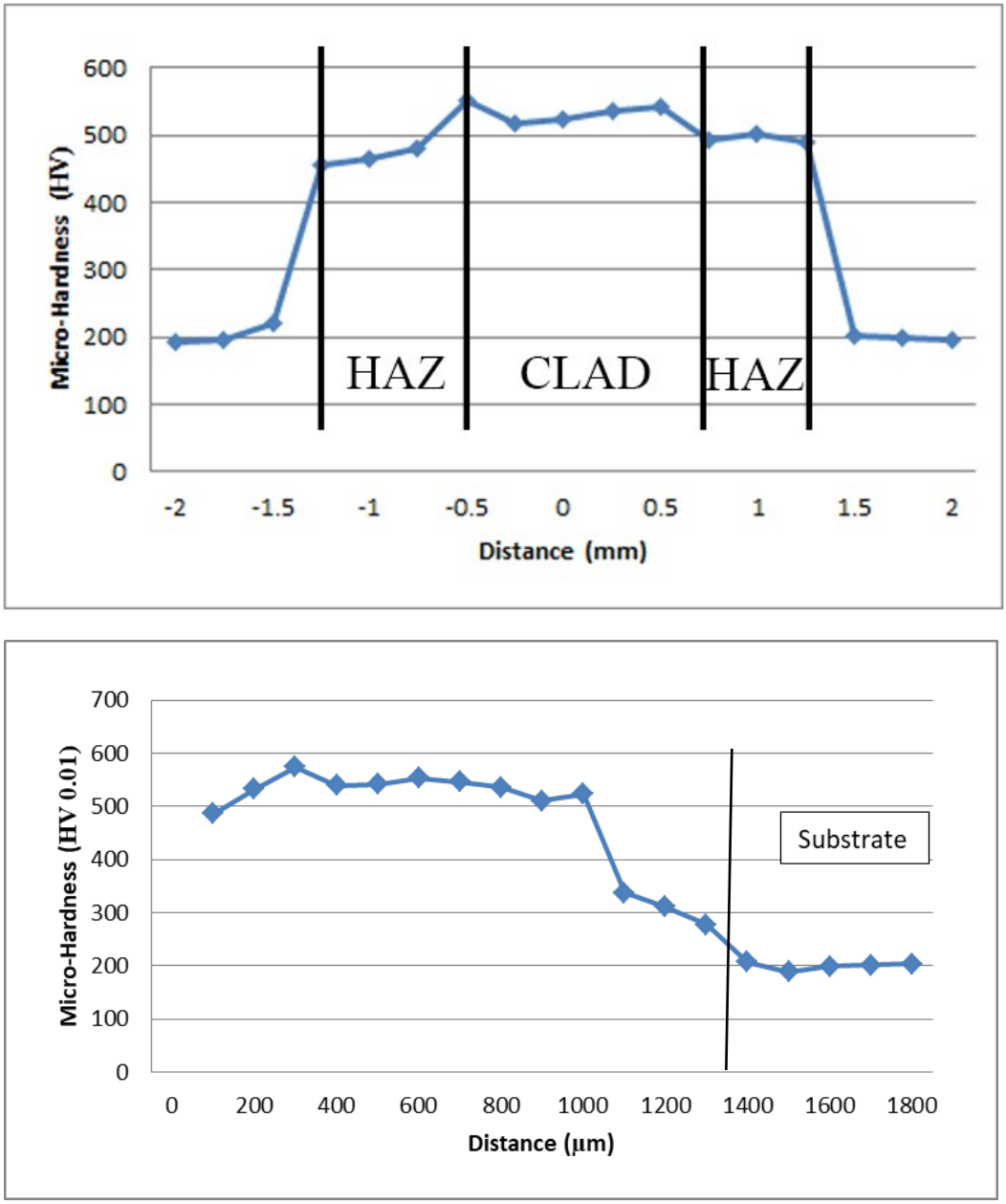

Figure 12. (a) Variation of micro-hardness in cross-section of cladded specimen, (b) micro-hardness along with the depth of cladded layer and substrate.

4. Conclusion

In this article, the cladding of H13 hot work steel with Stellite 6 powder was investigated. The laser beam was used for melting Stellite 6 powder. The main results can be listed as follows.

- The laser power is the most important parameter of the height and width of the cladding layer and the dilution ratio. By increasing the laser power, the height and width of the cladding layer and dilution ratio increased.

- By increasing scanning speed and powder feed rate, the height and width of the cladded layer and the dilution ratio decreased.
- The best cladding condition was obtained by 300 W laser power, 150 mm/min scanning speed, 30 g/min powder feed rate, and 10% lateral overlapping of the scanning process.
- A considerable increase in surface hardness (164% increase) was obtained by laser cladding.
- The laser cladding of Stellite 6 powder on the H13 tool steel was carried out successfully and the proper condition for cladding a layer is determined. The cladded layer prepares good thickness and good dilution with higher hardness.

Compliance with Ethical Standards

Authors hereby announce that no part of this study was funded by any institutions and /or organizations. The authors also acknowledge no conflict of interest.

References

[1] Javid Y, Ghoreishi M and Torkamany M J 2015 Preplaced laser cladding of WC powder on Inconel 718 by laser. *Modares Mech. Eng.* 15: 98–106.

[2] Naghiyan Fesharaki M, Shoja-Razavi R, Mansouri H and Jamali H 2018 Microstructure investigation of Inconel 625 coating obtained by laser cladding and TIG cladding methods. *Surf. Coat. Tech.* 353: 25–31, https://doi.org/10.1016/j.surfcoat.2018.08.061.

[3] Moradi M, Arabi H and Kaplan A F H 2018 An experimental investigation of the effects of diode laser surface hardening of AISI 410 stainless steel and comparison with furnace hardening heat treatment. *J. Braz. Soc. Mech. Sci.* 41: 434, https://doi.org/10.1007/s40430-019-1925-2.

[4] Bhatnagar S, Mullick S and Gopinath M 2021 A lumped parametric analytical model for predicting molten pool temperature and clad geometry in pre-placed powder laser cladding. *Optik* 247: 168015, https://doi.org/10.1016/j.ijleo.2021.168015.

[5] Wu S, Liu Z, Huang X, Wu Y and Gong Y 2021 Process parameter optimization and EBSD analysis of Ni60A-25% WC laser cladding. *Int. J. Refract. Met. H.* 101: 105675, https://doi.org/10.1016/j.ijrmhm.2021.105675.

[6] Liu S S, Zhang M, Zhao G L, Wang X H and Wang J F 2022 Microstructure and properties of ceramic particle reinforced FeCoNiCrMnTi high entropy alloy laser cladding coating. *Intermetallics* 140: 107402, https://doi.org/10.1016/j.intermet.2021.107402.

[7] Yang J, Bai B, Ke H, Cui Z, Liu Z, Zhou Z, Xu H, Xiao J, Liu Q and Li H 2021 Effect of metallurgical behavior on microstructure and properties of FeCrMoMn

coatings prepared by high-speed laser cladding. *Opt. Laser Technol.* 144: 107431, https://doi.org/10.1016/j.optlastec.2021.107431.

[8] Lizzul L, Sorgato M, Bertolini R, Ghiotti A, Bruschi S, Fabbro F and Rech S 2021 On the influence of laser cladding parameters and number of deposited layers on as-built and machined AISI H13 tool steel multilayered claddings. *CIRP J. Manuf. Sci. Technol.* 35: 361–370, https://doi.org/10.1016/j.cirpj.2021.07.003.

[9] Cheng Q, Guo N, Fu Y, Wang G, Yu M and He J 2021 Investigation on in-situ laser cladding 5356 aluminum alloy coating on 5052 aluminum alloy substrate in water environment. J. Mater. Res. Technol. 15: 4343–4352, https://doi.org/10.1016/j.jmrt.2021.10.073.

[10] Karmakar D P, Muvvala G and Nath A K 2021 High-temperature abrasive wear characteristics of H13 steel modified by laser remelting and cladded with Stellite 6 and Stellite 6/30% WC. *Surf. Coat. Tech.* 422: 127498, https://doi.org/10.1016/j.surfcoat.2021.127498.

[11] Karmakar D P, Muvvala G and Nath A K 2020 Effect of scan strategy and heat input on the shear strength of laser cladded Stellite 21 layers on AISI H13 tool steel in as-deposited and heat treated conditions. *Surf. Coat. Tech.* 384: 25331, https://doi.org/10.1016/j.surfcoat.2019.125331.

[12] Lu J Z, Xue K N, Lu H F, Xing F and Luo K Y 2021 Laser shock wave-induced wear property improvement and formation mechanism of laser cladding Ni25 coating on H13 tool steel. J. Mater. Process. Tech. 296: 117202, https://doi.org/10.1016/j.jmatprotec.2021.117202.

[13] Telasang G, Dutta Majumdar J, Padmanabham G, Tak M and Manna I 2014 Effect of laser parameters on microstructure and hardness of laser clad and tempered AISI H13 tool steel. *Surf. Coat. Tech.* 258: 1108–1118, https://doi.org/10.1016/j.surfcoat.2014.07.023.

[14] Hao J, Hu F, Le X, Liu H, Yang H and Han J 2021 Microstructure and high-temperature wear behaviour of Inconel 625 multi-layer cladding prepared on H13 mould steel by a hybrid additive manufacturing method. *J. Mater. Process. Tech.* 291: 117036, https://doi.org/10.1016/j.jmatprotec.2020.117036.

[15] Lei Y, Sun R, Tang Y and Niu W 2015 Microstructure and phase transformations in laser clad CrxSy/Ni coating on H13 steel. *Opt. Laser. Eng.* 66: 181–186, https://doi.org/10.1016/j.optlaseng.2014.09.006.

[16] Xue K N, Lu H F, Luo K Y, Cui C Y, Yao J H, Xing F and Lu J Z 2020 Effects of Ni25 transitional layer on microstructural evolution and wear property of laser clad composite coating on H13 tool steel. *Surf. Coat. Tech.* 402: 126488, https://doi.org/10.1016/j.surfcoat.2020.126488.

[17] Kattire P, Paul S, Singh R and Yan W 2015 Experimental characterization of laser cladding of CPM 9V on H13 tool steel for die repair applications. *J. Manuf. Process.* 20: 492–499, https://doi.org/10.1016/j.jmapro.2015.06.018.

[18] Bagci E and Aykut Ş 2006 A study of Taguchi optimization method for identifying optimum surface roughness in CNC face milling of cobalt-based alloy (stellite 6). *Int. J. Adv. Manuf. Technol.* 29: 940–947, https://doi.org/10.1007/s00170-005-2616-y.

[19] Moradi M, Ashoori A and Hasani A 2020 Additive manufacturing of stellite 6 superalloy by direct laser metal deposition – Part 1: Effects of laser power and focal plane position. *Opt. Laser Technol.* 131: 106328, https://doi.org/10.1016/j.optlastec.2020.106328.

[20] Choo H, Sham K L, Bohling J, Ngo A, Xiao X, Ren Y, Depond P J, Matthews M J and Garlea E 2019 Effect of laser power on defect, texture, and microstructure of a laser powder bed fusion processed 316L stainless steel. *Mater. Design.* 164: 107534, https://doi.org/10.1016/j.matdes.2018.12.006.